RSC Advances

PAPER

View Article Online
View Journal | View Issue

Cite this: *RSC Adv.*, 2018, **8**, 14669

Liposomes formed from photo-cleavable phospholipids: *in situ* formation and photo-induced enhancement in permeability†

Dawei Zhang,[ab] Zhenzhen Liu,[a] Danielle Konetski,[a] Chen Wang,[a] Brady. T. Worrell[a] and Christopher N. Bowman *[ab]

Received 9th January 2018
Accepted 5th April 2018

DOI: 10.1039/c8ra00247a

rsc.li/rsc-advances

Photocleavable liposomes were formed *in situ* through the coupling of an *o*-nitrobenzyl-containing azide tail precursor and an alkyne-functionalized lysolipid by the copper-catalyzed azide–alkyne cycloaddition (CuAAC) reaction. Inclusion of the photolabile *o*-nitrobenzyl-structure enables control over the permeability and morphology of the liposomes. Photolysis of the *o*-nitrobenzyl group changes the molecular structure of the photolabile phospholipids, inducing phase transitions and permeability increases in the bilayer membrane, ultimately disrupting the liposome entity.

Introduction

Phospholipids are amphiphilic lipid molecules found in living tissues and comprise one of the predominant components of cell membranes,[1] a self-assembling bilayer structure. The ability of some phospholipids to assemble into liposomes, *i.e.* enclosed membrane structures, either alone or in the presence of cholesterol, makes them suitable for a wide array of potential applications including their use as a simplified artificial cell-model in biology-related research,[2–4] nano- and micro-reactors,[5] bio-imaging vehicles,[6] and drug delivery systems (DDS).[7–9]

In the pursuit of this simplified cell-model, researchers have introduced functions into liposomes, aiming to mimic various "smart" behaviors of the cell and to realize practical applications. In particular, liposomes composed of phospholipids have been investigated as potential drug delivery systems (DDS) for the loading and release of drug molecules. Characteristics of a successful DDS are stability, specific targeting and controlled release,[10] making "smart" or "controllable" liposomal DDS an important topic. Controlled release requires rapid cargo-release from the delivery vehicle, triggered by the application of certain stimuli, such as pH changes,[11–13] molecular recognition,[14,15] temperature,[16] magnetic field,[17,18] or light.[19–22] Of these options, light is of significant interest because it enables both spatial and temporal control of the process.

Natural phospholipids are not photo-responsive, so photo-responsive functionalities are often introduced into molecular structures to prepare photo-responsive liposomes. Bayer *et al.* creatively designed a phosphotidylcholine lipid with an *o*-nitrobenzyl-structure beside the glycerol-linker, and liposomes formed by this functionalized phospholipids exhibit significant photo-responsiveness.[23] Other approaches utilizes the chemically reactive group of natural phospholipids to introduce photo-responsive functionalities in liposomes, such as the primary amine head group of phosphotidylethanolamine.[24] In addition to the difficulties in purification of zwitterionic molecules in these approaches, the photo-responsive phospholipids are unable to assemble into vesicular structure. This issue often necessitates inclusion of other natural phospholipids to form a liposome matrix in which the photo-responsive phospholipids are inserted. Unfortunately, addition of matrix-phospholipids can lead to a change in response kinetics and extent. In the research of photo-responsive DDS, liposomes with excellent photo-responsive kinetics and extent are important in both fundamental studies and in application-oriented research. In addition to the spatial and temporal control afforded by irradiation, the light exposure provides a non-invasive trigger to induce property changes in liposomes such as a phase-transition in the bilayer membrane, permeability enhancements and shape changes.[25,26] Practically, a rapid photo-responsiveness enhances the spatial and temporal control associated with the use of light to facilitate enhanced response in DDS. Thus, an ideal photo-responsive liposome-based DDS should be composed of phospholipids which are chemically modified to have rapid photo-responsiveness while preserving the ability to self-assemble into liposomes, rather than embedding photo-responsive molecules into the matrix liposome.[27]

Herein, we have developed such a method for the facile preparation of photo-responsive liposomes by synthesizing molecular structures that enable *in situ* click chemistry for phospholipid formation and subsequent self-assembly in one

[a]*Department of Chemical and Biological Engineering, University of Colorado, UCB 596, Boulder, Colorado 80309, USA. E-mail: christopher.bowman@colorado.edu*
[b]*Materials Science and Engineering Program, University of Colorado Boulder, USA*

† Electronic supplementary information (ESI) available. See DOI: 10.1039/c8ra00247a

pot. This design was inspired by the work of Budin *et al.* which mimics cell membrane formation using a "click" chemical reaction.[28] A clickable aliphatic azide precursor containing a photolabile *o*-nitrobenzyl structure was synthesized with high yield and an alkyne functionalized lysolipid was prepared with a minor modification of the previously reported procedure.[28] The two precursors were coupled by the copper-catalyzed azide–alkyne cycloaddition (CuAAC) reaction in aqueous conditions using a sodium ascorbate and $CuSO_4$ catalyst system, resulting in triazole and nitrobenzyl-containing phosphatidylcholine (TNBPC) molecules. These phospholipids self-assemble into liposomes *in situ*. In TNBPC-liposomes, photolysis of the *o*-nitrobenzyl structure cleaves one hydrophobic chain from the TNBPC molecule, inducing a permeability increase of the bilayer membrane and eventually causing disruption of the liposome (Scheme 1).

Experimental

General procedure

All reactions were performed under air. All chemical reagents were obtained commercially without further purification. ^1H and ^{13}C NMR spectra were recorded on a Bruker Avance-III 400 spectrometer. Fourier Transform Infrared (FTIR) spectra were recorded on a Nicolet 670 FT-IR spectrometer. Ultraviolet-Visible spectra were recorded on a UV-Vis spectrophotometer (Thermo-Fischer Scientific). Fluorescence excitation ratios were recorded on a QM-6 steady-state spectrofluorimeter (Photon Technology International). Fluorescence images were recorded on a Zeiss Axiovert 200M Wide field microscope equipped with an EMCCD Camera. Phase transition in bilayer membrane of liposomes was recorded on an Olympus polarized optical microscope equipped with a 530 nm full wavelength retardation wave-plate.

In situ preparation of liposomes

1-(5-dodecyloxy-2-nitrophenyl) ethyl-2-azido ethyl carbonate (NBN_3) (1.16 mg, 2.5 μmol) and alkyne lysolipid (1.44 mg, 2.5 μmol) were completely dispersed in water (500 μL) by ultrasound and stirring. $CuSO_4$ (0.12 mg, 0.75 μmol) and sodium ascorbate (0.5 mg, 2.5 μmol) were added into the dispersion, and vortexed for 30 seconds, then the reaction vial was placed statically for 24 hours.

LC-MS monitoring of CuAAC coupling

CuAAC coupling was performed as described above. A 10 μL sample was taken from the reaction system at different times. After dilution with 50 μL methanol, samples were analyzed by LC-MS coupled with an evaporative light scattering detector (ELSD). For all LC-MS runs, the flow-rate was 1 mL min^{-1} and elution-phase consisted of HPLC-grade water with 0.1% formic acid and HPLC-grade methanol with 0.1% formic acid.

NMR monitoring of triazole-phospholipid formation and self-assembly of liposomes

CuAAC coupling and simultaneous assembly of liposomes were performed in deuterium oxide, increasing the concentration of the two precursors to 20 mmol L^{-1}, and NMR-spectra were recorded before adding $CuSO_4$ and sodium ascorbate. After addition of catalysts, NMR-spectra were recorded at different times. The NMR-scanning mode was water-suppression.

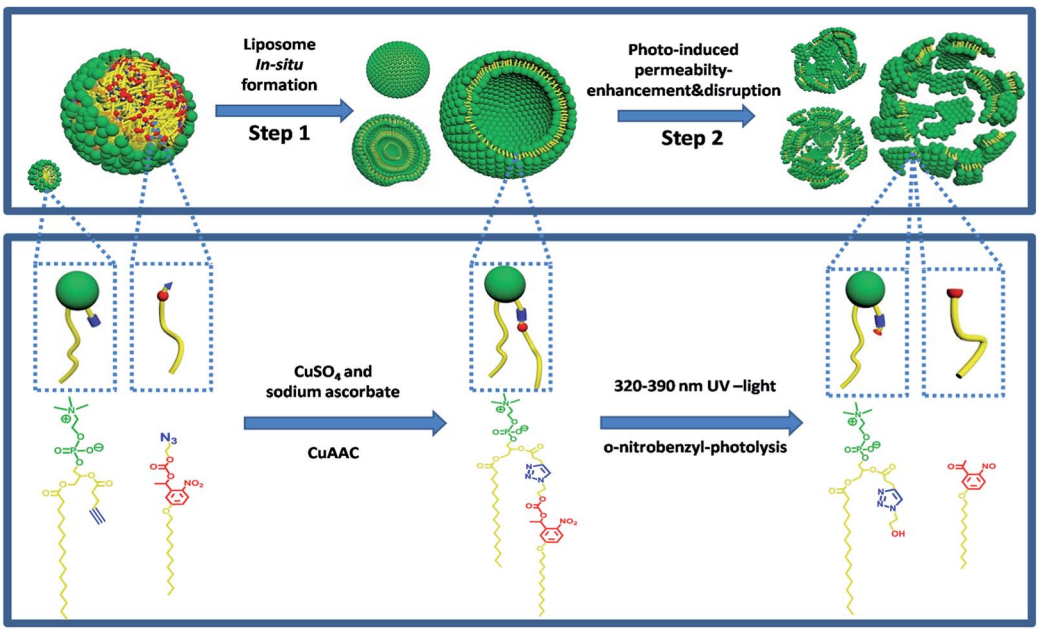

Scheme 1 An emulsion of lipid precursors aggregates into micelles and stabilized oil droplets. In step 1, the CuAAC reaction between precursors results in the production of TNBPC molecules which self-assemble into liposomes. In step 2, photolysis of the *o*-nitrobenzyl structure cleaves one aliphatic chain from the phospholipid structure, causing change in aggregation-morphology and phase-transition of the bilayer membrane, inducing a permeability-increase in the membrane and eventual disruption of the liposomes.

Microscopy imaging of *in situ* liposome formation and photo-induced liposome disruption

For imaging of *in situ* liposome formation, 200 μL precursor water-dispersion (AL&NBN_3 or AL&BN_3) with rhodamine DHPE (5 μmol L^{-1}) as the fluorescent dye were injected into a chamber on a glass slide and imaged by fluorescence microscopy. Certain amounts of $CuSO_4$ and sodium ascorbate aqueous solutions were injected into the chamber in sequence. Fluorescence images were recorded every 30 s at various points. For imaging of photo-induced liposome disruption, 10 μL of liposome dispersion (TBNPC- or TBPC-liposomes) were dropped onto a slide and covered by a glass-slip, half of which was totally shielded by foil-paper. On the microscope, two points were selected separately in the covered and uncovered areas. After turning on a 365 nm-light, fluorescence images were recorded in sequence every 1 minute at the selected points.

Polarized optical microscopy imaging of phase transition in bilayer membrane of liposomes under UV exposure

Liposomes sample under UV exposure was observed using an Olympus polarized optical microscope (POM) equipped with a 530 nm full wavelength retardation wave-plate.

Ratiometric fluorescence assay

Preparation of liposomes loading HPTS. Precursors were dispersed in HEPES buffer (10 mM, pH = 7.04) containing 1 mM HPTS as well as $CuSO_4$ and sodium ascorbate to trigger CuAAC coupling and liposome assembly. After 20 hours, extra liposomal components were removed by size exclusive chromatography (Sepharose 4B, Sigma-Aldrich) eluted with 10 mM HEPES, pH = 7.04. The eluted fraction containing HPTS-loaded liposomes was collected and used within 48 hours.

Measurement of membrane permeability with HPTS assay. 50 μL of liposomes loaded with HPTS was added to 1900 μL HEPES buffer in a fluorescence cuvette (10 mm × 10 mm) with gentle vibration. After measurements of the excitation-ratio R (λ_{em} = 510 nm, λ_{ex} = 410 nm, λ_{ex} = 453 nm, $R = (I_{410ex}/I_{453ex})_{510em}$) were collected 5 times over 8 minutes, 10 μL NaOH (0.5 M) were added into the cuvette with gentle vibration. Cuvettes were irradiated with 320–390 nm UV-light and measured at fixed time points. After 80 minutes of consistent measurements, samples were sonicated for 20 minutes, then the final excitation-ratio (R) was measured. The permeability increase at each time point was calculated using the equation:

$$\text{Permeability increase} = \frac{R_t - R_0}{R_\infty - R_0} \times 100\%$$

where R_0 = average R before NaOH addition, $R_\infty = R$ after 20 minutes of sonication, $R_t = R$ at certain time point.

Results and discussion

Monitoring of CuAAC and observation of *in situ* liposome formation

The *in situ* liposome formation was confirmed by monitoring the CuAAC reaction using HPLC-ELSD and NMR, while the generated vesicular structures were observed using fluorescence microscopy. The CuAAC mediated formation of phospholipids was observed between alkyne lysolipid (AL) and *o*-nitrobenzyl-azide (NBN_3) using HPLC-ELSD traces to reveal consumption of the two precursors and formation of TNBPC (Fig. 1a). This activity was further validated using ^{1}H NMR spectroscopy, where formation of the triazole-ring was confirmed by the appearance of a proton signal at 7.56 ppm (Fig. 1b). The process of *in situ* CuAAC-mediated liposome formation was explored by examining the changes in the ^{1}H NMR spectrum. In the spectrum of pure ALPC which well disperses into D_2O and assembles into micelles,[29] the singlet peaks at 0.93 ppm and 0.5 ppm are attributed to –CH_2– and –CH_3– signals in the aliphatic tail of ALPC (Fig. 1e dash black line). New –CH_2– and –CH_3– signals appear at 0.83 ppm and 0.44 ppm, respectively, after addition of NBN_3 (ALPC&NBN_3 mixture, 1 : 1 mole ratio), forming two doublet peaks with uneven intensity (Fig. 1e bold black line). Considering the insolubility of NBN_3 in D_2O, the appearance of peaks associated with the NBN_3 is due to the presence of ALPC which acts as a surfactant to solubilize NBN_3 in D_2O and to form the ALPC-stabilized NBN_3 oil droplets. During the CuAAC reaction, the intensity decrease of the peaks at 0.93 ppm and 0.5 ppm is caused by the consumption of ALPC, and eventually two slightly separated peaks with almost uniform intensity are formed (Fig. 1e pink line) and indicate liposome formation.[30] The methyl proton of the choline head group at 2.89 ppm gradually splits into two partially overlapping peaks (Fig. 1f), characteristic of curved bilayer membranes formed when the liposomes self-assemble.[30] Here, it should be pointed out that the overall broadening and weakening of the ^{1}H NMR signals was induced by formation of the bilayer membrane in which molecular mobility is restricted. Furthermore, time-lapse fluorescence microscopy provided direct observation during the formation of liposomes, during which bilayer membranes budded from the surface of AL and NBN_3 Oil-droplets and propagated into the aqueous environment (Video S1†).

To provide a negative control for photo-cleavage capabilities introduced into the phospholipid structure, another azide functionalized aliphatic tail was synthesized to include a benzyl moiety (BN3) in place of the *o*-nitrobenzyl group. In this control group (AL and BN3), the CuAAC reaction also proceeded to form liposomes from a triazole and benzyl containing phosphatidylcholine lipid (TBPC) (Video S2†). Between these two systems, we verified that TNBPC or TBPC molecules self-assemble into liposomes, indicating that triazole-rings and benzyl-rings in the hydrophobic tail region of phospholipid molecules do not affect their capability for liposome self-assembly.

Fluorescence imaging of photo-induced liposome disruption

In TNBPC-liposomes each building block contains one *o*-nitrobenzyl structure. Thus, photolysis of all the *o*-nitrobenzyl-structures in the liposomes cleaves one tail in each building block, and the change of chemical structure in all the TNBPC molecules has the potential to induce drastic changes in liposomal structure. To demonstrate that the photolysis of the *o*-nitrobenzyl-linker induces a morphological response in

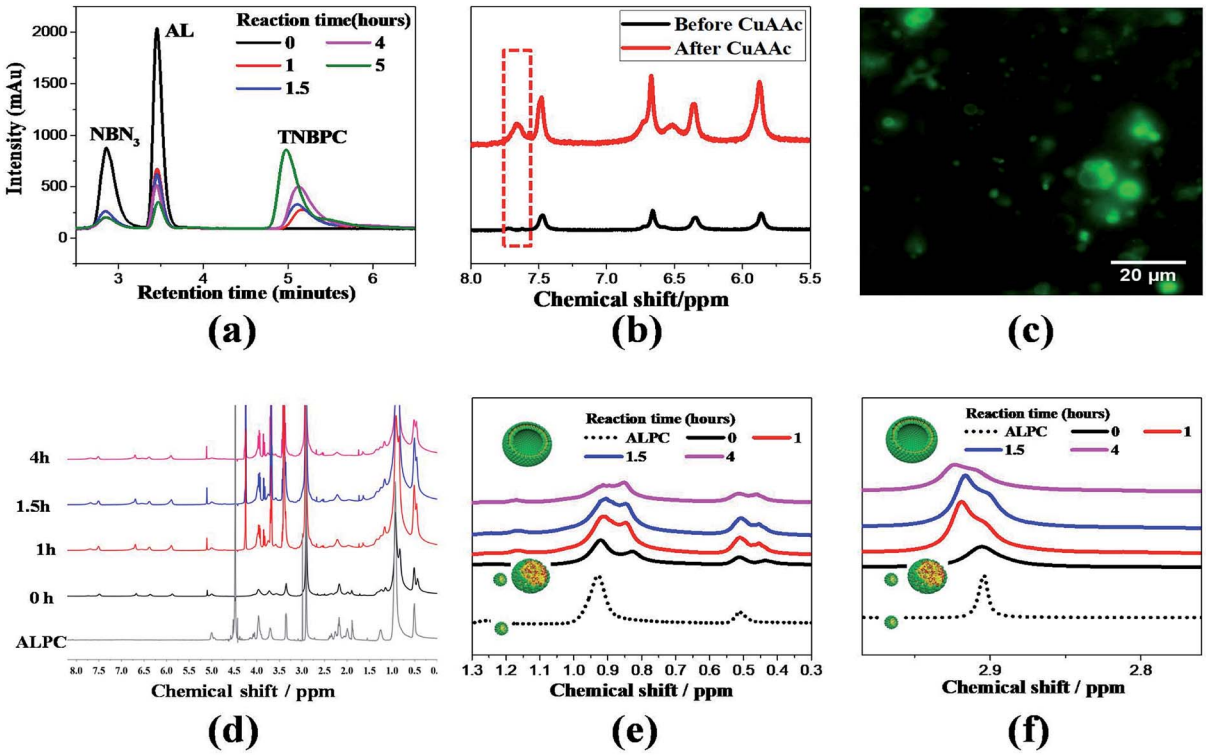

Fig. 1 (a) HPLC-ELSD traces indicate conversion of alkyne lysolipid (AL) and *o*-nitrobenzyl azide tail (NBN_3) to triazole phospholipid (TNBPC) in the presence of sodium ascorbate and $CuSO_4$. (b) ^{1}H NMR spectrum before and after CuAAC reaction, showing appearance of a triazole proton signal. (c) Fluorescence microscopy image shows liposomes after CuAAC reaction. (d) Waterfall overlapped ^{1}H NMR spectrums of alkyne lysolipid (ALPC) and ALPC&NBN_3 (1 : 1 mole ratio) over the course of the CuAAC reaction. (e) Expanded area in (d), splitting of the methyl proton signal at the choline head-group confirms liposome formation due to curvature changes from bilayer formation. (f) Expanded area in (d), intensity change of ^{1}H NMR signals of methylene ($-CH_2-$) and methyl ($-CH_3$) in aliphatic tails, showing the solubilisation of NBN_3 by ALPC (dash black → bold black), consumption of ALPC during CuAAC reaction (black → red → blue → pink), and eventually two splitted signals due to curvature change when liposomes formed (pink).

liposomes, we applied time-lapse fluorescence microscopy to observe the change in liposomes upon exposure to UV-light (Fig. 2). Under 365 nm UV-irradiation (10 mW cm^{-2}, 10 minutes), the TNBPC-liposomes were disrupted within 10 minutes (Video S3†) but liposomes remained unchanged in the absence of UV-light (Video S4†). To verify that the photo-induced changes were due to cleavage of the *o*-nitrobenzyl structure, UV-vis absorption spectra were taken showing spectral changes concurrent with liposome disruption (Fig. S3†). In the control formulation, the TBPC-liposomes had no obvious extensive morphological change upon exposure to UV-light, but some liposome clusters were observed to fuse with each other (Video S5†). This observation was in accordance with previous research which demonstrated that UV-light exposure can cause undulation of the bilayer membranes and induce liposomal fusion,[31] as was in fact observed in both populations. When irradiation was continued, the TBPC-liposomes had no further morphological changes while the TNBPC-liposomes started to collapse and disappear. This obvious difference in photo-responsiveness was attributed-to the photolysis of the *o*-nitrobenzyl structure.

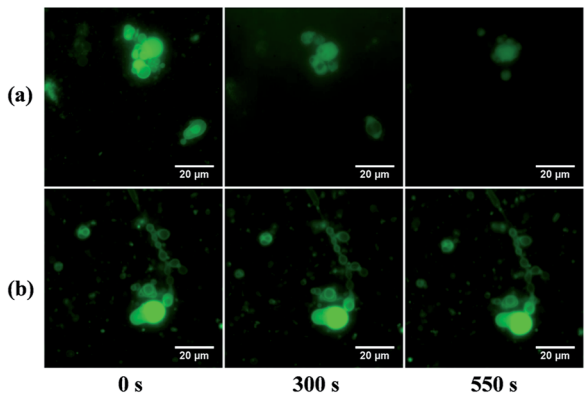

Fig. 2 Fluorescence microscopy images of TNBPC-liposomes with (a) and without (b) UV-irradiation. Under UV-light (365 nm, 10 mW cm^{-2}) for 300 seconds, liposomes fused and underwent morphological change. After 550 seconds of irradiation, some liposomes collapsed and disappeared. Without UV-light, liposomes had no change.

Observation of phase transitions in bilayer membrane over the course of photo-induced liposome disruption

According to our original molecular design, photolysis of the *o*-nitrobenzyl structure cleaves one hydrophobic tail from TNBPC molecules, regenerating a lysolipid structure and producing

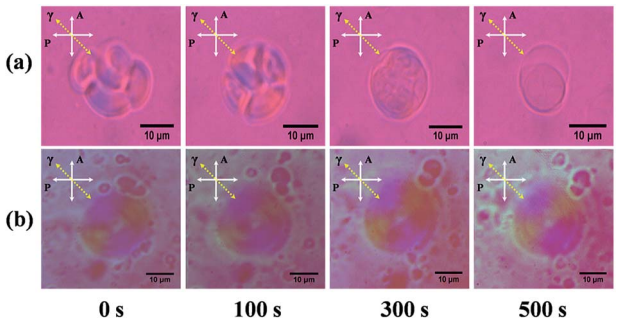

Fig. 3 Polarized optical microscopy (POM) images of liposome under UV exposure (365 nm, 10 mW cm^{-2}, 10 minutes), P: polarizer, A: analyzer, γ: a full wavelength (530 nm) retardation wave-plate with slow axis marked with yellow dash arrow. (a). TNBPC-liposome. Images show the gradual disappearance of birefringence of bilayer membrane, confirming the perturbation of liquid crystal phase in the bilayer structure. (b) TBPC-liposome images show no change in the interference colours, indicating no perturbation of molecule-alignment in bilayer membrane.

nitroso-benzophenone tails. The cleaved lipids have different hydrophilic/hydrophobic ratios from the TNBPC molecules and will change the assembly morphology. In particular, the cleaved hydrophobic tails do not prefer an aligned state and are prone to induce a phase-transition in the bilayer membrane. To verify the existence of a phase transition in the bilayer membrane during photo-induced disruption of the liposomes, we applied a polarized optical microscope (POM) with a full wavelength retardation (530 nm) wave-plate to observe the change of birefringence of TNBPC-liposomes under UV exposure. Due to the molecular similarity of TNBPC with natural phosphotidylcholine, the structure of the bilayer membrane of TNBPC-liposomes should be analogous to that of the cell membrane, in which the aliphatic hydrocarbon tails of TNBPCs are aligned, and the regular molecular alignment in the bilayer membranes forms a liquid crystal phase and shows weak optical anisotropy, or birefringence.[32] POM images confirm birefringence in the bilayer membrane of TNBPC-liposomes (Fig. 3), showing yellow and blue interference colours.[33] As shown in Fig. 3a, during the photo-induced disruption of TNBPC-liposomes (365 nm, 10 mW cm^{-2}, 10 minutes), the liposome morphology changed, but still maintained a certain contour profile before complete disruption, otherwise the interference colours of the liposome kept disappearing during 365 nm UV-irradiation. The disappearance of interference colours indicates loss of birefringence, which confirms the perturbation of the liquid crystal phase of the bilayer membrane of the TNBPC-liposomes. In the control group, the TBPC-liposome had no change in interference colours upon UV irradiation, indicating the structural integrity of the bilayer membrane (Fig. 3b). This microscopy observation verifies the existence of a phase transition in the process of photo-induced disruption of TNBPC-liposomes, and indicates that the photolysis of nitrobenzyl structure in TNBPC molecules, which causes structural change of TNBPCs, triggers the phase transition in bilayer membrane.

Permeability enhancement of the membrane of TNBPC liposomes by photo-induced phase transition

The demonstration of the existence of a phase transition arouses one question in the permeability change of membrane of TNBPC-liposomes in the process of photo-induced disruption. To investigate the permeability change of bilayer membranes during the photo-induced disruption, we applied a ratiometric fluorescence assay to characterize the bilayer membrane permeability upon UV-light irradiation using the pH-sensitive fluorescent probe 8-hydroxy-1,3,6-pyrenetrisulfonate (HPTS) as the loading molecule in liposomes.[34,35] Results revealed that under 320–390 nm UV-light exposure (10 mW cm^{-2}, 80 minutes), the TNBPC-liposome permeability was enhanced 70% in 60 minutes, two times faster than that of the control group (TBPC-liposomes) in which permeability enhancement was only 35% (Fig. 4A). The permeability curve for the TBPC-liposomes indicates that UV light induces leakage in the bilayer membrane even in the absence of photo-cleavable moieties. Combining these results with microscopy observations of the TBPC-liposomes under UV-light, this apparent leakage was probably caused by the fusion of liposomes. Furthermore, the permeability enhancement of the liposomes with the *o*-nitrobenzyl moiety lags behind the photolysis. Permeability increased less than 5% in the first 10 minutes of UV irradiation despite photolysis reaching 60%, as indicated by UV-Vis. The most probable explanation for this outcome is that even though tail-cleavage has been triggered in some TNBPC molecules, uncleaved TNBPCs still maintain the bilayer structure and liposomal morphology, and the change of assembly morphology and phase transition need time to proceed, resulting in a lag time between permeability enhancement of the liposome and photolysis of the *o*-nitrobenzyl structure. It is important to note, however, that photolysis of the *o*-nitrobenzyl structure is the driving force behind the permeability enhancement.

We anchored cholesterol within the bilayer membrane of liposomes. Ratiometric fluorescence assays in which each of the liposomal samples (TNBPC and TBPC) were doped with cholesterol indicated that each formulation was more stable

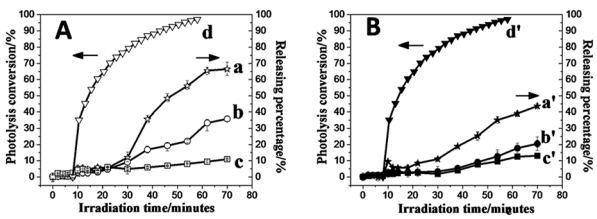

Fig. 4 Liposome permeability increase curves under UV-light and photolysis conversion curve of *o*-nitrobenzyl-structure in TNBPC (320–390 nm, 10 mW cm^{-2}, 80 minutes). (A) No cholesterol group, (a) TNBPC-liposomes with UV exposure, (b) TBPC-liposomes with UV exposure, (c) TBPC-liposomes without UV exposure, and (d) photolysis conversion curve of the *o*-nitrobenzyl structure in TNBPC. (B) With cholesterol group (10 mol% to AL), (a′) TNBPC-liposomes with UV exposure. (b′) TBPC-liposomes with UV exposure, (c′) TBPC-liposomes without UV exposure, and (d′) photolysis–conversion curve of the *o*-nitrobenzyl-structure in TNBPC.

under UV exposure (Fig. 4B). During one-hour UV irradiation, the permeability increased by 45% and 20% for TNBPC-liposomes and TBPC-liposomes, respectively. This change was attributed to the ability of cholesterol to stabilize the lipid bilayers and smooth the phase transition. With respect to the influence of tail length on the liposome permeability and its sensitivity to irradiation, it is expected that if the photosensitive tails were shortened, the bilayer membrane would be expected to be more permeable both before and after irradiation, due to a lower gel-transition temperature resulting from the short aliphatic chains.[36] As such, it is expected that the length of the photo-responsive tail could provide an additional handle with which to control the photosensitivity and permeability changes.

Conclusions

In summary, we prepared photo-cleavable liposomes by an *in situ* method. Artificial phospholipid molecules containing triazole and *o*-nitrobenzyl moieties self-assembled into liposomes upon formation *via* CuAAC reaction. The photolysis of the *o*-nitrobenzyl structure upon exposure to UV light induced phase transition of the membrane and enhanced permeability of the bilayer membrane, ultimately resulting in liposomal disruption. While the CuAAC reaction is used here as a means for triggering liposome-formation and introducing the photo-cleavable moiety into liposomes, this reaction is known to be problematic for use with living cells due to the presence of copper. It is readily envisioned that a variety of other click reactions could similarly be applied to assemble photosensitive phospholipids and to trigger liposome-formation, and subsequently be used to engender a photosensitive permeability increase. This *in situ* liposome formation method combining the precursor design and click reaction provides a versatile and powerful method to prepare photo-responsive liposomes.

Conflicts of interest

There is no conflict to declare.

Acknowledgements

This work was supported by the U.S. Army Research Office (MURI program, Award W911NF-13-1-0383). The fluorescent imaging work was performed at the BioFrontiers Institute Advanced Light Microscopy Core at University of Colorado Boulder. We thank Prof. Neal K. Devaraj at the University of California San Diego for result discussion, Prof. Ivan Smalyukh and Dr Qingkun Liu at the Univeristy of Colorado Boulder for assistance in POM, Dr Annette Erbse at University of Colorado Boulder for assistance in fluorescence spectrometry, and Dr Joseph Dragavon for assistance in fluorescence microscopy.

Notes and references

1 W. E. M. Lands, *Biochim. Biophys. Acta, Mol. Cell Biol. Lipids*, 2000, **1483**, 1–14.
2 A. D. Bangham and R. W. Horne, *J. Mol. Biol.*, 1964, **8**, 660–IN610.
3 Y. Elani, R. V. Law and O. Ces, *Nat. Commun.*, 2014, **5**, 5305.
4 P. Walde, H. Umakoshi, P. Stano and F. Mavelli, *Chem. Commun.*, 2014, **50**, 10177–10197.
5 K. Renggli, P. Baumann, K. Langowska, O. Onaca, N. Bruns and W. Meier, *Adv. Funct. Mater.*, 2011, **21**, 1241–1259.
6 M. L. Matteucci and D. E. Thrall, *Vet. Radiol. Ultrasound*, 2000, **41**, 100–107.
7 T. M. Allen and P. R. Cullis, *Science*, 2004, **303**, 1818–1822.
8 A. Samad, Y. Sultana and M. Aqil, *Curr. Drug Del.*, 2007, **4**, 297–305.
9 E. Soussan, S. Cassel, M. Blanzat and I. Rico-Lattes, *Angew. Chem., Int. Ed.*, 2009, **48**, 274–288.
10 T. M. Allen and P. R. Cullis, *Adv. Drug Del. Rev.*, 2013, **65**, 36–48.
11 W. Chen, F. Meng, R. Cheng and Z. Zhong, *J. Controlled Release*, 2010, **142**, 40–46.
12 D. C. Drummond, M. Zignani and J.-C. Leroux, *Prog. Lipid Res.*, 2000, **39**, 409–460.
13 D. Zhang, H. Zhang, J. Nie and J. Yang, *Polym. Int.*, 2010, **59**, 967–974.
14 F. J. Martin, W. L. Hubbell and D. Papahadjopoulos, *Biochemistry*, 1981, **20**, 4229–4238.
15 R. R. Sawant and V. P. Torchilin, *AAPS J.*, 2012, **14**, 303–315.
16 N. D. Winter, R. K. Murphy, T. V. O'Halloran and G. C. Schatz, *J. Liposome Res.*, 2011, **21**, 106–115.
17 S.-L. Huang and R. C. MacDonald, *Biochim. Biophys. Acta, Biomembr.*, 2004, **1665**, 134–141.
18 E. Viroonchatapan, H. Sato, M. Ueno, I. Adachi, K. Tazawa and I. Horikoshi, *Life Sci.*, 1996, **58**, 2251–2261.
19 A. S. Derycke and P. A. de Witte, *Adv. Drug Del. Rev.*, 2004, **56**, 17–30.
20 P. Shum, J.-M. Kim and D. H. Thompson, *Adv. Drug Del. Rev.*, 2001, **53**, 273–284.
21 A. Yavlovich, A. Singh, R. Blumenthal and A. Puri, *Biochim. Biophys. Acta, Biomembr.*, 2011, **1808**, 117–126.
22 A. Yavlovich, B. Smith, K. Gupta, R. Blumenthal and A. Puri, *Mol. Membr. Biol.*, 2010, **27**, 364–381.
23 A. M. Bayer, S. Alam, S. I. Mattern-Schain and M. D. Best, *Chem.–Eur. J.*, 2014, **20**, 3350–3357.
24 A. G. Kohli, P. H. Kierstead, V. J. Venditto, C. L. Walsh and F. C. Szoka, *J. Controlled Release*, 2014, **190**, 274–287.
25 J. Yuan, S. M. Hira, G. F. Strouse and L. S. Hirst, *J. Am. Chem. Soc.*, 2008, **130**, 2067–2072.
26 Y. Sun, Y. Ji, H. Yu, D. Wang, M. Cao and J. Wang, *RSC Adv.*, 2016, **6**, 81245–81249.
27 R. M. Uda, E. Hiraishi, R. Ohnishi, Y. Nakahara and K. Kimura, *Langmuir*, 2010, **26**, 5444–5450.
28 I. Budin and N. K. Devaraj, *J. Am. Chem. Soc.*, 2012, **134**, 751.
29 R. J. Brea, C. M. Cole and N. K. Devaraj, *Angew. Chem.*, 2014, **126**, 14326–14329.
30 C. G. Brouillette, J. P. Segrest, T. C. Ng and J. L. Jones, *Biochemistry*, 1982, **21**, 4569–4575.
31 S. Kulin, R. Kishore, K. Helmerson and L. Locascio, *Langmuir*, 2003, **19**, 8206–8210.

32 S. Bibi, R. Kaur, M. Henriksen-Lacey, S. E. McNeil, J. Wilkhu, E. Lattmann, D. Christensen, A. R. Mohammed and Y. Perrie, *Int. J. Pharm.*, 2011, **417**, 138–150.
33 D. S. Miller, R. J. Carlton, P. C. Mushenheim and N. L. Abbott, *Langmuir*, 2013, **29**, 3154–3169.
34 A. Hennig, L. Fischer, G. Guichard and S. Matile, *J. Am. Chem. Soc.*, 2009, **131**, 16889–16895.
35 T. Liu, C. Bao, H. Wang, L. Fei, R. Yang, Y. Long and L. Zhu, *New J. Chem.*, 2014, **38**, 3507–3513.
36 M. Blok, E. Van der Neut-Kok, L. Van Deenen and J. De Gier, *Biochim. Biophys. Acta, Biomembr.*, 1975, **406**, 187–196.